

Article

Investigating the Distribution of Intimin and Invasin in *Aeromonas hydrophila* and Their Role in Host Tissue Attachment

Agradi Bhattacharyya¹, Goutam Banerjee^{2,*} and Pritam Chattopadhyay^{3,*} 

¹ Raja Rammohun Roy Mahavidyalaya, Radhanagar, Nangulpara, Hooghly, West Bengal 712406, India; agradi@bhattacharyya@gmail.com

² Department of Food Science and Human Nutrition, University of Illinois at Urbana-Champaign, Urbana, IL 61801, USA

³ M.U.C. Women's College, Burdwan, Purba-Bardhaman, West Bengal 713104, India

* Correspondence: goutamb@illinois.edu or banerjee.goutam2@gmail.com (G.B.); pritamb@biotechnol@gmail.com (P.C.)

Abstract: *Background:* *Aeromonas hydrophila* is a key pathogen affecting freshwater fish, including *Labeo rohita* (rohu), causing significant aquaculture losses. This study explores the role of intimin and invasin, known virulence factors, in *A. hydrophila* pathogenesis using in silico methods. *Methods:* We analyzed the distribution of invasin and intimin across 53 *A. hydrophila* genomes and examined their physicochemical properties, secondary structures, and 3D models. Since crystal structures were unavailable, homology-based modeling was employed to study the structure of rohu β -integrins. In silico docking was performed to explore the interactions between intimin/invasin and β -integrins. *Results:* Our findings revealed that intimin and invasin were present in only 6 out of the 53 *A. hydrophila* strains examined, which were designated as hypervirulent strains. The transmembrane regions of intimin and invasin were modeled as β -barrels, a common feature of porins. The in silico docking experiments indicated the significant binding affinity of invasin and intimin with all the β -integrins of rohu fish, suggesting a critical role in host attachment and cellular internalization. *Conclusions:* This in silico study highlights the pivotal role of invasin and intimin in host tissue's binding efficacy, offering valuable insights into the binding potential of *A. hydrophila* across various organs in rohu fish.



Academic Editor: Bart C. Weimer

Received: 6 December 2024

Revised: 14 January 2025

Accepted: 24 January 2025

Published: 2 February 2025

Citation: Bhattacharyya, A.; Banerjee, G.; Chattopadhyay, P. Investigating the Distribution of Intimin and Invasin in *Aeromonas hydrophila* and Their Role in Host Tissue Attachment. *Bacteria* **2025**, *4*, 7. <https://doi.org/10.3390/bacteria4010007>

Copyright: © 2025 by the authors. Licensee MDPI, Basel, Switzerland. This article is an open access article distributed under the terms and conditions of the Creative Commons Attribution (CC BY) license (<https://creativecommons.org/licenses/by/4.0/>).

Keywords: *A. hydrophila*; invasin; intimin; homology modeling; β -integrins; docking

1. Introduction

Bacterial diseases pose one of the most serious threats to the lives of fish, both in the wild and in captivity. Diseases can spread rapidly through water, often leading to severe health issues for fish populations. In this direction, *Aeromonas hydrophila* is recognized as a versatile fish pathogen that can have catastrophic consequences for the aquaculture industry [1]. Infections in fish can manifest primarily as ulcerative dermatitis [2], septicemia [3], necrotizing fasciitis [4], piknosis, and necrotic damage in the spleen and kidney [5]. *A. hydrophila* is responsible for various conditions, including gill degeneration in *Oreochromis niloticus* [6], hepato-pancreatic infection in *Ictalurus punctatus* [7], bilateral exophthalmia in *Pangasianodon hypophthalmus* [8], visceral hemorrhagic septicemia in *Acipenser sinensis* [9], and many more. Additionally, *A. hydrophila* is associated with Aeromonad red sore disease and epizootic ulcerative syndrome in carp and other fish [10], underscoring its versatility as a pathogen in aquatic environments.

The autotransporter-3 (AT-3) family of adhesins are the outer membrane (OM) proteins known as intimin/invasin (Int/Inv) and are present in pathogenic *E. coli* (Int), *Yersinia* sp. (Inv), and other proteobacteria strains [11]. Invasins are monomeric autotransporters (type 3) [12] and promote pathogen translocation on target cells [13]. Furthermore, the invasin of *Y. pseudotuberculosis* binds to β 1-integrin superfamily proteins on the surfaces of eukaryotic host cells and triggers the rearrangement of the host cell cytoskeleton and the internalization of bacteria [14]. Meanwhile, in *Salmonella enterica*, invasin plays a key role in promoting bacterial attachment and the penetration of host cells [15]. Similarly, another bacterial outer membrane adhesin, called intimin, promotes *Escherichia coli*'s adhesion to intestinal villi in calves and the production of AE lesions [16]. As with invasins, intimins are also monomeric autotransporters [12] that promote the adhesion or invasion of *Salmonella enterica* in vertebrate host cells [15]. According to Fairman et al. (2012), both invasins and intimins act as central virulence factors in attaching and effacing lesions (AE lesions), as they can bind to host cells through their C-terminal extracellular domains, while their N-terminal β -domains are embedded in the outer bacterial membrane [17].

On the other hand, integrins ($\alpha\beta$ -heterodimeric integral proteins) belong to the cell adhesion receptor superfamily of eukaryotic hosts and are recognized to bind proteins containing the specific sequence Arg-Gly-Asp or RGD [18]. Fish, as vertebrates, have eight different β -integrins [19]. Ligand recognition by integrins is primarily mediated by a cationic binding site on the β -integrin, adjacent to the exposed α -integrin [20]. Bacteria have been shown to interact, either directly or indirectly, with integrins, facilitated by a surface-localized ligand encoded by the pathogen [21]. Previous research has reported that several pathogenic bacteria, like *Shigella* and *Yersinia*, bind to integrin β 1 on host cells, facilitating invasion and infection [22,23]. It has also been reported that the ligands of some fish integrins contain negatively charged amino acids (Asp or Glu) that are directly involved in receptor binding [24]. Additionally, integrin overexpression has been linked to increased bacterial adhesion and infection in blackwater teleosts [25].

Despite the significance of *A. hydrophila* as a fish pathogen, there is limited information about its autotransporter type 3 proteins, invasin and intimin, and their interactions with fish during disease establishment. In this investigation, we studied the distribution of invasin and intimin across all available *A. hydrophila* genomes. Since tertiary protein structures for *A. hydrophila* invasin/intimin and rohu β -integrins were unavailable, homology modeling was conducted. Finally, the interactions between invasin/intimin and fish β -integrins were elucidated through in silico docking experiments.

2. Materials and Methods

2.1. Data Acquisition from Different Databases

The nucleotide sequences for two key test proteins, invasin (AHA_1064) and intimin (AHA_1066), were retrieved from the KEGG Orthology database (<https://www.genome.jp/kegg/ko.html> last accessed on 31 March 2024) (Table S1). Similarly, the protein sequences of invasin and intimin, along with the β -integrins (β 1– β 8) from *Labeo rohita* (rohu), were obtained from the UniProt database (<https://www.uniprot.org/> last accessed on 31 March 2024). In addition, the *A. hydrophila* genome sequences were sourced from the NCBI Genome database (<https://www.ncbi.nlm.nih.gov/genome> last accessed on 31 March 2024), a well-established resource for complete genome sequences. All datasets were accessed and collected on or before 31 March 2024, ensuring that the latest available sequence information was included in the analyses.

2.2. Distribution of Invasin and Intimin Proteins Within *A. hydrophila* Genomes

We conducted microbial genome BLAST searches using the tBLASTn algorithm (Table S2) to investigate the distribution of the invasin (AHA_1064) and intimin (AHA_1066) proteins across *A. hydrophila* genomes. To further explore the synteny (the conserved order of genes) between the invasin and intimin genes and their neighboring regions in different *A. hydrophila* genomes, we used the SyntTax server [26]. All analyses were performed using online tools and databases accessed on or before 31 March 2024.

2.3. Prediction of Physicochemical Properties of Invasin, Intimin, and β -Integrins

The physicochemical properties of the test proteins (invasin and intimin) (Table 1) and β -integrins (Table 2) were predicted using the ExPASy-ProtParam server (<https://web.expasy.org/protparam/> last accessed on 31 March 2024). These properties included the amino acid composition, molecular weight, extinction coefficient, aliphatic index, instability index, grand average hydropathy (GRAVY), isoelectric point, molecular formula, total number of atoms, and charged residues.

Table 1. Physicochemical properties of the test proteins selected for this study.

Physicochemical Parameter	Invasin	Intimin
Number of amino acids	916	535
Molecular weight	99,614.99	56,335.50
Extinction coefficient (EC)	127,325 M/cm	54,110 M/cm
Aliphatic index (AI)	83.08	85.83
Instability index (II)	29.18	25.02
Grand average of hydropathicity (GRAVY)	−0.327	−0.106
Isoelectric point (pI)	4.77	4.42
Molecular formula	C ₄₃₉₉ H ₆₈₆₄ N ₁₂₁₈ O ₁₃₉₉ S ₁₃	C ₂₄₅₅ H ₃₈₈₃ N ₆₇₁ O ₈₂₄ S ₁₁
Total number of atoms	13893	7844
Number of positively charged residues (Arg + Lys)	73	30
Number of negatively charged residues (Asp + Glu)	116	59

2.4. Secondary Structure Characterization

The CYS_REC tool (<http://www.softberry.com/> last accessed on 31 March 2024) was used to predict disulfide bonds, bonding patterns, and the number of cysteine residues. Additionally, the SOPMA tool (https://npsa-prabi.ibcp.fr/cgi-bin/npsa_automat.pl?page=/NPSA/npsa_sopma.html last accessed on 31 March 2024) was used to predict the secondary structures of the *A. hydrophila* intimin and invasin (Table S3), along with rohu fish β -integrins (Table S4).

2.5. Functional Analysis (Disulfide Bonds, Number of Cysteine Residues, and Configuration) of Invasin, Intimin, and β -Integrins

The properties of the test proteins were analyzed using the SOSUI server (http://harrier.nagahama-i-bio.ac.jp/sosui/sosui_submit.html last accessed on 31 March 2024). Additionally, functional analyses were conducted for both the test proteins (Table S5) and β -integrins (Table S6), focusing on their potential roles in cellular adhesion, signaling, and interactions with other molecules.

Table 2. Physicochemical properties of the rohu β -integrins.

Proteins Selected for This Study	No. of Amino Acids	Molecular Weight	Extinction Coefficient (EC)	Aliphatic Index (AI)	Instability Index (II)	Grand Average of Hydropathicity (GRAVY)	Isoelectric Point (pI)	Molecular Formula	Total No. of Atoms	No. of Positively Charged Residues (Arg + Lys)	No. of Negatively Charged Residues (Asp + Glu)
β 1	801	88,914.58	62,415	73.87	43.11	−0.410	6.56	C ₃₈₃₉ H ₆₁₁₉ N ₁₀₇₉ O ₁₂₀₃ S ₇₁	12,311	98	101
β 2	767	84,690.43	66,425	70.90	32.88	−0.410	6.13	C ₃₆₄₉ H ₅₇₇₈ N ₁₀₃₀ O ₁₁₄₈ S ₇₀	11,675	89	96
β 3	783	85,889.65	80,740	77.52	44.62	−0.219	5.25	C ₃₇₇₆ H ₅₉₅₄ N ₁₀₅₆ O ₁₁₉₃ S ₆₈	11,845	77	100
β 4	1930	214,581.74	201,340	73.87	43.08	−0.460	5.77	C ₉₃₇₆ H ₁₄₇₉₇ N ₂₆₀₅ O ₂₉₄₆ S ₁₀₇	29,831	211	237
β 5	805	89,154.62	69,865	73.53	46.39	−0.275	6.28	C ₃₈₅₄ H ₆₀₇₁ N ₁₀₈₉ O ₁₁₉₅ S ₇₄	12,283	88	96
β 6	779	85,424.44	64,810	78.31	45.60	−0.105	5.05	C ₃₇₁₁ H ₅₈₁₇ N ₁₀₀₇ O ₁₁₅₉ S ₇₃	11,767	97	68
β 7	768	85,263.04	65,145	77.41	39.63	−0.347	6.09	C ₃₆₈₀ H ₅₈₄₆ N ₁₀₃₆ O ₁₁₆₁ S ₆₅	11,788	86	96
β 8	816	90,464.26	85,655	72.30	42.13	−0.355	5.63	C ₃₈₉₇ H ₆₁₀₂ N ₁₁₂₄ O ₁₂₂₂ S ₆₉	12,414	81	104

2.6. Homology Modeling and Evaluation of the Tertiary Structure

The 3D structure of the test proteins was predicted using the SWISS-MODEL server. First, structural templates were identified using the ExpASY web server (<https://swissmodel.expasy.org/> last accessed on 31 March 2024), and the target sequences were aligned with these templates accordingly. The SWISS-MODEL server was then used to construct the protein models and perform an initial quality assessment. To ensure the accuracy and reliability of the predicted 3D structures, the models were further evaluated using multiple analytical tools, including (a) RAMPAGE [27], (b) the ProQ web server (<https://proq.bioinfo.se/cgi-bin/ProQ/ProQ.cgi> last accessed on 31 March 2024), (c) the ProSA web server (<https://prosa.services.came.sbg.ac.at/prosa.php> last accessed on 31 March 2024), and (d) Ramachandran plot analysis [28]. The tertiary structures of the test proteins (Table S7) and rohu β -integrins (Table S8) were also evaluated accordingly.

2.7. In Silico Protein–Protein Docking

We used HDock servers to investigate protein–protein docking interactions. HDock (<http://hdock.phys.hust.edu.cn/> last accessed on 31 March 2024) employs a hybrid approach combining template-based modeling and ab initio free docking for protein–protein interactions. HDock accepts amino acid sequences or PDB files as input and integrates experimental data, such as binding site residues on the receptor or ligand or small-angle X-ray scattering (SAXS) data, into the global docking process to predict the binding complexes between two proteins automatically. The docking score was determined using the iterative scoring function ITScorePP. A score of around −200 or better, along with a confidence score exceeding 0.7, signifies a high likelihood of successful docking [29].

3. Results

3.1. Distribution of Invasin and Intimin within *A. hydrophila* Strains

The tBLASTn analysis revealed the presence of invasin and intimin in only six strains (ATCC 7966, GSH8-2, LP0103, WCX23, WP8-S18-ESBL-02, and 23-C-23) out of the 53 *A. hydrophila* genomes examined (Table S2). The synteny analysis further validated their exclusive occurrence in these six strains (Figure 1).

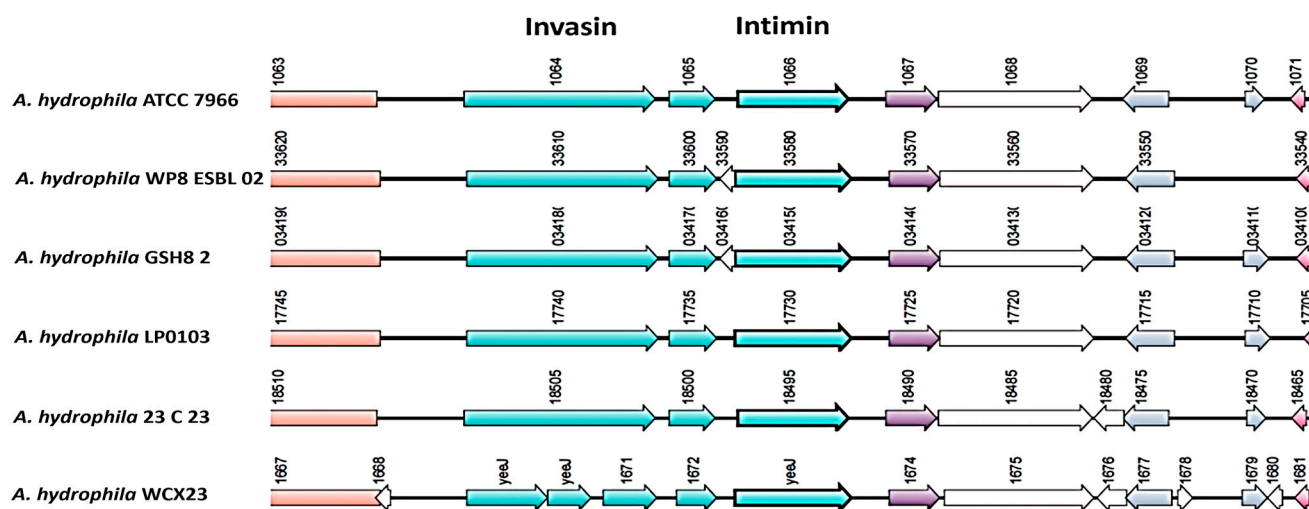


Figure 1. Synteny of invasin and intimin within the *A. hydrophila* genomes.

3.2. Physicochemical Properties of Invasin, Intimin, and Rohu β -Integrins

At 280 nm, the enzyme commission (EC) values of the proteins invasin and intimin were found to be 12,732 and 54,110 M/cm, respectively (Table 1). Invasin and intimin comprised 916 and 535 amino acids, respectively (Table 1). The pI value of invasin (4.77) was recorded to be higher than that of intimin (4.42) (Table 1). The total number of negative charge residues (Asp + Glu) in invasin and intimin was 116 and 59, respectively (Table 1). In contrast, the total quantity of positive charge residues (Arg + Lys) in invasin and intimin was 73 and 30, respectively. Invasin and intimin exhibited instability indices of 29.18 and 25.02, respectively (Table 1). The aliphatic index (AI) was estimated to be 83.08 for invasin and 85.83 for intimin (Table 1).

At 280 nm, the EC values of the rohu β -integrins (β 1– β 8) were found to be 62,415; 66,425; 80,740; 201,340; 69,865; 64,810; 65,145 and 85,655 M/cm, respectively (Table 2). The β -integrins comprised 801, 767, 783, 1930, 805, 779, 768, and 816 amino acids, respectively (Table 2). In the present investigation, the eight Rohu β -integrins could be arranged by the pI values in the following manner: β 1 > β 5 > β 2 > β 7 > β 4 > β 8 > β 3 > β 6. The total number of negatively charged residues (Asp + Glu) and positively charged residues (Arg + Lys) in β -integrins ranged from 68 to 237 and 77 to 211, respectively (Table 2). Additionally, the instability indices of these β -integrins ranged from 32.88 to 46.39. The AI values for β 1, β 2, β 3, β 4, β 5, β 6, β 7, and β 8 were 73.87; 70.90; 77.52; 73.87; 73.53; 78.31; 77.41 and 72.30, respectively (Table 2).

3.3. Functional Analysis of Invasin, Intimin, and Rohu β -Integrins

The functional analysis of invasin and intimin was carried out and presented elsewhere (Table S5). Intimin lacks disulfide bonds. However, only two cysteines and a single disulfide bond were recorded in the invasin of *Aeromonas hydrophila* (Table S5). On the other hand, 58 cysteines and 24 disulfide bonds, 59 cysteines and 22 disulfide bonds, 56 cysteines and 32 disulfide bonds, 64 cysteines and 22 disulfide bonds, 59 cysteines and 26 disulfide bonds,

57 cysteines and 25 disulfide bonds, 55 cysteines and 26 disulfide bonds, and 55 cysteines and 22 disulfide bonds were recorded in the rohu β -integrins (β 1 to β 8), respectively (Table S6).

3.4. Secondary Structure Characterization of Invasin, Intimin, and Rohu β -Integrins

The secondary structure analysis revealed that the alpha helix constituted 9.72% of the *A. hydrophila* invasin protein, while intimin exhibited significantly lower alpha helix content of only 0.19% (Table S3). Regarding the composition of extended strands, invasin and intimin exhibited values of 25.66% and 29.35%, respectively. Furthermore, approximately 64.63% of invasin and 70.47% of intimin were classified as random coils. Notably, neither of these proteins exhibited any beta turns, as illustrated in Figure S1A,B.

In contrast, the β -integrins demonstrated greater variability in the secondary structure composition across different integrins (β 1 to β 8). For example, the alpha helix percentage of β -integrins varied from 11.40% to 23.16% (Table S4). The extended strand compositions of the integrins were as follows: β 1: 14.73%, β 2: 15.12%, β 3: 15.96%, β 4: 23.99%, β 5: 16.27%, β 6: 17.46%, β 7: 16.02%, and β 8: 14.46% (Table S4). The random coil content for each integrin was as follows: β 1: 64.79%, β 2: 63.89%, β 3: 62.58%, β 4: 64.61%, β 5: 63.35%, β 6: 60.85%, β 7: 61.72%, and β 8: 63.38% (Figure S2a–h).

3.5. Homology Modeling of Invasin, Intimin, and Rohu β -Integrins

The 3D models of invasin and intimin (obtained from *A. hydrophila* ATCC 7966) were built using the following templates: A0A3T1A166.1.A for invasin (Figure 2A, GMQE score 0.72) and A0A4P7IWM0.1.A for intimin (Figure 2B, GMQE score 0.91) (Table S7). The transmembrane regions of these outer membrane proteins were predicted to form β -barrel structures, a hallmark characteristic of porins (Figure 2A,B). The C-terminal domain of invasin and intimin shares structural similarity with C-type lectin-like domains (CTLDs). Conversely, the outer membrane portions of invasin and intimin were characterized by a composition of α -helices, extended strands, and random coils, but notably lacked any β -turns (Figure 2A,B). The NH₂-terminal domains of invasin (D1–D5) and intimin (D1–D3) resemble the folds of the eukaryotic immunoglobulin superfamily (IgSF), yet they lack disulfide bonds and conserved core residues (Figure 2A,B). Additionally, the extracellular segment of intimin includes an extra Ig-like domain, referred to as D0 (Figure 2B).

The most similar 3D models of the β -integrins (β 1 to β 8) of rohu fish were generated using the SWISS-MODEL server based on the best matching sequences (Table S8). The following templates were used for model construction: β 1: A0A286Y9W0.1.A (GMQE score: 0.87) (Figure S3a), β 2: E7FCN5.1.A (GMQE score: 0.86) (Figure S3b), β 3: B3DIP9.1.A (GMQE score: 0.84) (Figure S3c), β 4: F1RA51.1.A (GMQE score: 0.71) (Figure S3d), β 5: F1QF91.1.A (GMQE score: 0.83) (Figure S3e), β 6: F1QGX0.1.A (GMQE score: 0.84) (Figure S3f), β 7: E7F4H9.1.A (GMQE score: 0.84) (Figure S3g), β 8: A0A7J6C0U9.1.A (GMQE score: 0.73) (Figure S3h).

3.6. Evaluation of Tertiary Structures of Invasin, Intimin, and Rohu β -Integrins

In the Ramachandran plot analysis (Figure 3c), the residues in the favored regions of the invasin and intimin proteins of *A. hydrophila* constituted 94.31% and 95.16%, respectively (Table S9). Meanwhile, the analysis obtained via the ProQ server revealed that the predicted LG scores of invasin and intimin of *A. hydrophila* were 11.489 and 10.667, respectively. The MaxSub values were -0.871 for invasin and -1.691 for intimin, further supporting the quality of the predicted structures. The ProSA server analysis revealed Z-scores of -1.691 and -0.871 for intimin and invasin of *A. hydrophila*, respectively (Table S9). The sequence positions of intimin and invasin were analyzed, revealing a mixture of hydrophobic and hydrophilic regions that correlated with their functional domains. Similarly, the structural

validation and quality assessment of the predicted rohu β -integrins (β 1– β 8) models were performed (Table S10). The results from the ProSA web validation are presented in three formats (Figure S4a–h). In the Ramachandran plot analysis, the residues in the favored regions for the β -integrins (β 1– β 8) amounted to 96.25%, 96.60%, 96.07%, 87.71%, 94.27%, 95.11%, 94.46%, and 92.80%, respectively (Figure S4a–h). The ProQ server revealed LG scores of 9.647, 11.038, 11.218, -0.835 , 10.442, 9.884, 10.113, and 9.409 for β 1– β 8, respectively. The MaxSub values were -0.548 , -0.659 , -0.751 , -0.113 , -0.594 , -0.517 , -0.599 , and -0.463 for β 1– β 8, respectively.

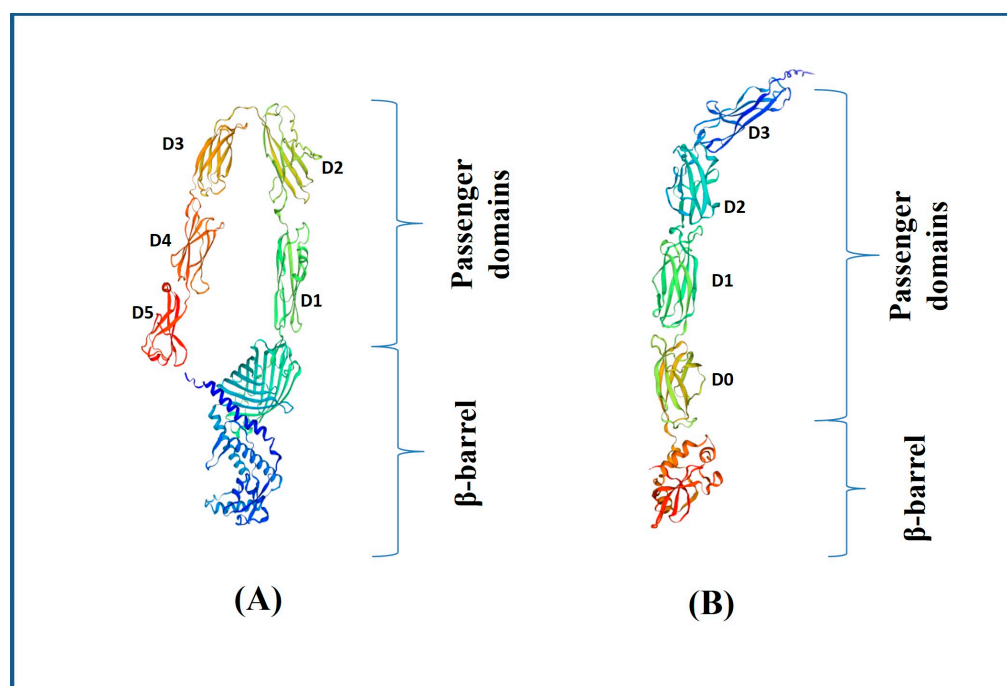


Figure 2. Homology modeling of the (A) invasin and (B) intimin of *A. hydrophila* ATCC 7966 by SWISS-MODEL, accessed via the ExPASy web server.

3.7. Molecular Docking of Invasin and Intimin with Rohu Integrins

The key residues of invasin involved in integrin binding include positions 903–913, which form helix 1 and its adjacent loop in domain D5. The best docking models were selected based on the interactions between integrin, intimin, and the rohu β -integrins, using the docking scores (Figure 4A,B).

The docking quality was evaluated through the docking scores, confidence scores (Table 3), and ligand RMSDs (Table S11). The docking scores ranged from -405.89 to -246.23 , while the confidence scores varied from 0.8734 to 0.9832. The RMSDs of the residue pairs within 5.0 Å between the receptor and ligand are detailed in Table S11. For instance, Thr 894 of invasin (D5) interacts with Gln 626 of integrin β 1 (Figure 5A), and Tyr 39 of intimin (D3) interacts with Met 689 of integrin β 1 (Figure 5B). The full residue interactions and RMSD values for all docking models are provided in Table S11.

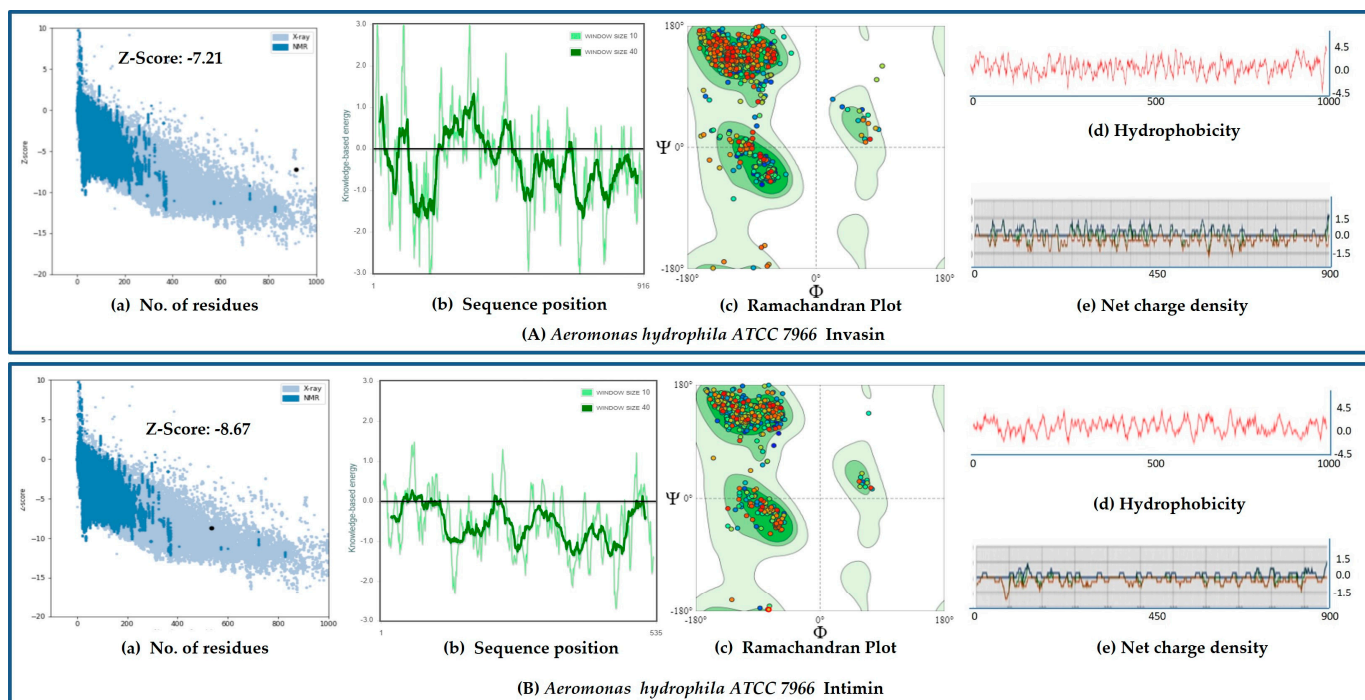


Figure 3. Evaluation of tertiary structures of the (A) invasin and (B) intimin of *A. hydrophila* ATCC 7966. In each panel, (a) represents the Z-scores in terms of residues, (b) represents the sequence position, (c) represents the Ramachandran plot, (d) represents the hydrophobicity, and (e) represents the net charge density.

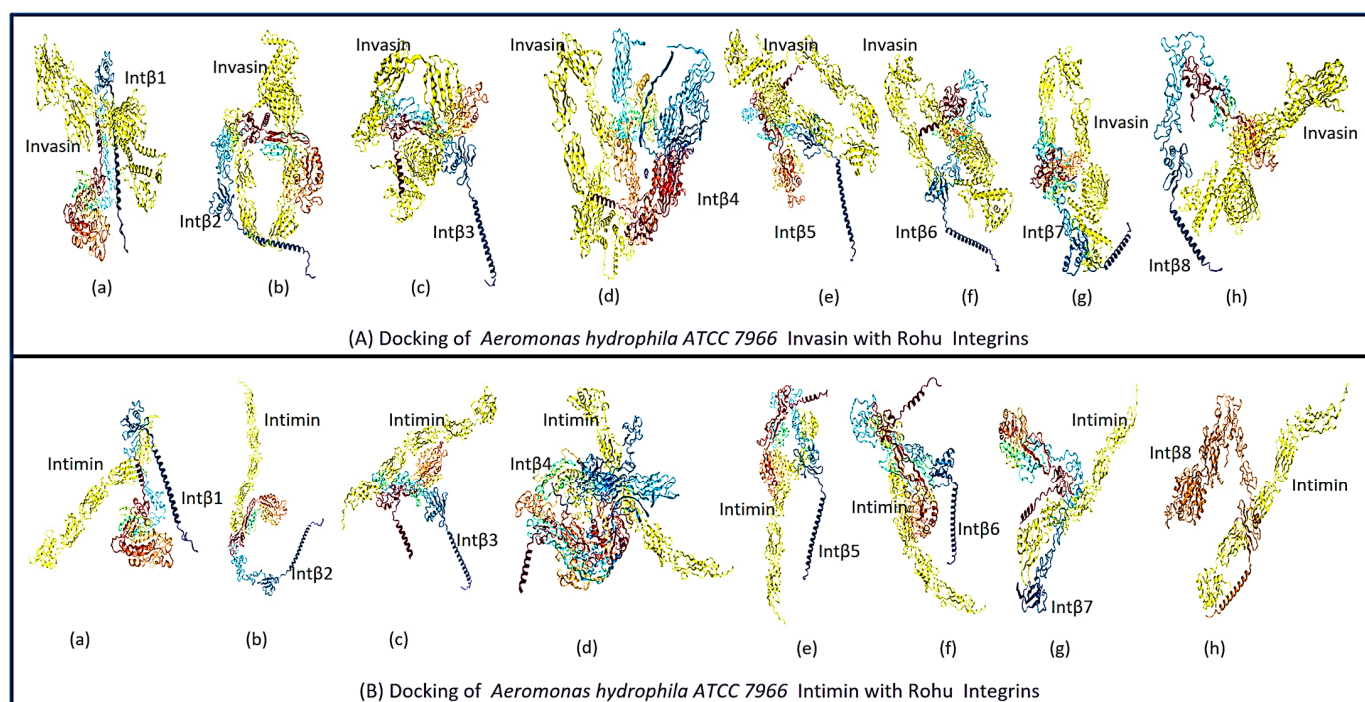
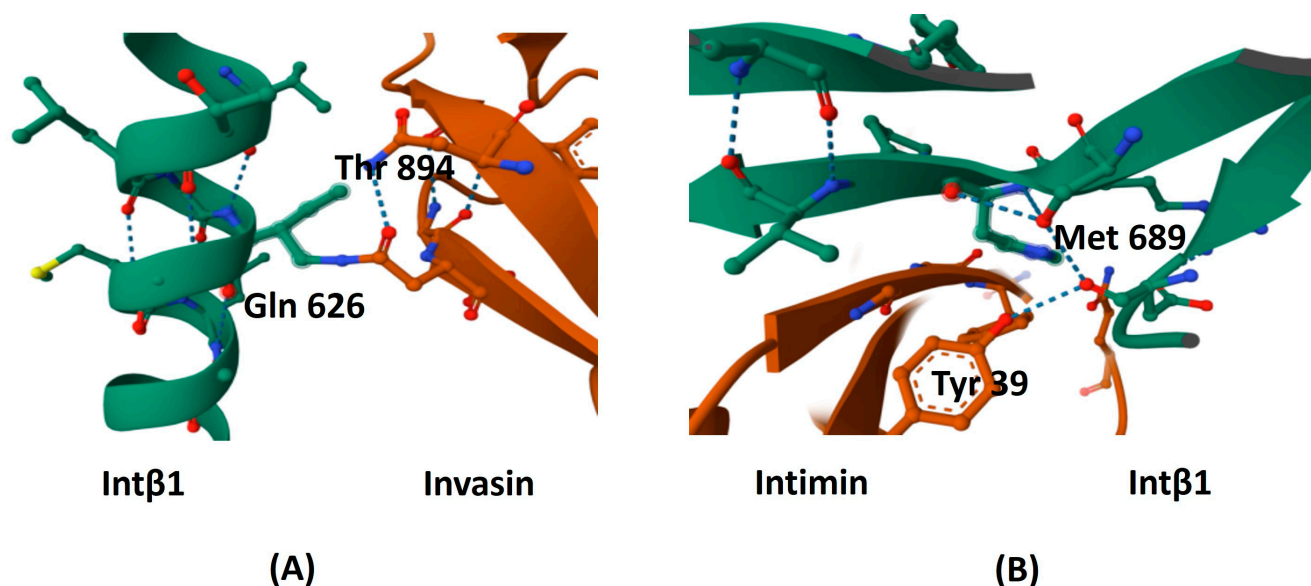


Figure 4. Molecular docking of the (A) invasin and (B) intimin proteins of *A. hydrophila* ATCC 7966 with the β -integrins of *L. rohita*. In each panel (A,B), (a) to (h) indicate the docking of a particular test protein with integrins β 1 to β 8.

Table 3. Results of the docking of the test proteins (invasin and intimin) with eight different human β -integrins.

Integrin Receptor (Rohu)	Ligand (<i>A. hydrophila</i>)	Docking Score	Confidence Score
Integrin β 1	Invasin	−332.28	0.9746
	Intimin	−264.23	0.9076
Integrin β 2	Invasin	−298.53	0.9512
	Intimin	−246.59	0.8734
Integrin β 3	Invasin	−318.39	0.9667
	Intimin	−246.32	0.8729
Integrin β 4	Invasin	−353.40	0.9832
	Intimin	−307.06	0.9586
Integrin β 5	Invasin	−320.60	0.9681
	Intimin	−261.00	0.9020
Integrin β 6	Invasin	−405.89	0.9940
	Intimin	−261.00	0.9020
Integrin β 7	Invasin	−330.12	0.9735
	Intimin	−250.01	0.8808
Integrin β 8	Invasin	−330.12	0.9735
	Intimin	−259.63	0.8996

**Figure 5.** Examples of interacting amino acid residues within the docking models: (A) Thr 894 of invasin (D5) interacts with Gln 626 of integrin β 1, and (B) Tyr 39 of intimin (D3) interacts with Met 689 of integrin β 1.

4. Discussion

4.1. Limited Distribution of Invasin and Intimin Within *A. hydrophila* Strains

Invasins and intimins play a critical role in bacterial pathogenesis by facilitating the attachment of bacteria to host epithelial surfaces [30]. Previous studies have reported that invasins and intimin proteins are primarily associated with γ -proteobacteria, including *Hafnia alvei*, *Citrobacter rodentium*, enteropathogenic and enterohaemorrhagic *Escherichia coli*, and enteropathogenic *Yersinia* spp. [31,32]. However, in this study, invasins and intimins were identified in only six strains of *A. hydrophila* (ATCC 7966, GSH8-2, LP0103, WCX23, WP8-S18-ESBL-02, and 23-C-23) out of the 53 genomes analyzed (Table S2). Interestingly, all these strains are known to be hypervirulent [33,34]. The limited presence of invasins and intimins in specific strains highlights their significance in the evolutionary adaptation of *A. hydrophila*, particularly in relation to virulence and pathogenicity. For example, the absence of an intimin-like protein in a uropathogenic *E. coli* pathogenicity island has been linked

to reduced inflammation and pathogenic potential [35]. Similarly, an invasin-like adhesin (*InvL*) is critical for *Acinetobacter baumannii* in uropathogenesis [36].

4.2. Mapping of *A. hydrophila* Invasin and Intimin Within Bacterial Chromosome

Tsai et al. (2010) reported that *A. hydrophila* carries an Ahy1 protein, which is classified within the invasin/intimin family, playing a role in bacterial adherence and the invasion of host cells [31]. In the present study, it was found that the invasin and intimin proteins of *A. hydrophila* are encoded in a single operon on the bacterial chromosome. Notably, invasin and intimin are encoded by the *inv* and *yeeJ* genes, respectively (Figure 1). For example, *Yersinia pseudotuberculosis* produces invasin through the chromosomal *inv* locus [37]. The *yeeJ* protein, previously identified in *E. coli* as an inverse autotransporter, binds to peptidoglycan in the bacterial cell wall, a function that is essential for biofilm formation. This capability enables bacteria to adhere to surfaces and resist environmental stressors. *yeeJ* plays a significant role in bacterial persistence, particularly in biofilm development, which is critical for pathogenicity and environmental survival [38]. In *E. coli*, approximately 35% of the reported genomes carry the *yeeJ* gene [39], highlighting its widespread presence and importance in bacterial ecology and infection mechanisms.

4.3. High Stability of Invasin and Intimin Within *A. hydrophila* Strains

The *A. hydrophila* invasin consists of 916 amino acids, with a molecular weight of 99,614.99 Da, whereas intimin is composed of 535 amino acids, with a molecular weight of 56,335.50 Da. For comparison, *Y. pseudotuberculosis* produces an invasin composed of 986 amino acids, which is encoded by the chromosomal *inv* locus [37]. Meanwhile, in *E. coli* K12 strains, full-length variants of intimin are expressed as intimin- α (939 amino acids), intimin- β (936 amino acids), or intimin- γ (934 amino acids) [40]. The analysis of the physicochemical properties of proteins is very important to assess their stability and structural integrity. For instance, *A. hydrophila*'s invasin and intimin exhibit high aliphatic index (AI) values of 83.08 and 85.83, respectively, reflecting their hydrophobic nature, which enhances proteins' stability. A previous study reported that a high AI value is a positive indicator of the thermal stability of proteins [41]. In contrast, both proteins display low instability indices (II) (intimin: 25.02; invasin: 29.18), which further suggests that they are stable proteins. Previous studies have indicated that the instability index (II) is an important factor in predicting protein stability, where a higher II value is associated with increased susceptibility to thermal degradation in the protein [42]. Furthermore, both proteins have a negative GRAVY score, indicating they are hydrophilic in nature [42], and they exhibit acidic PI values (intimin: 4.42; invasin: 4.77), reinforcing their stability [42] (Table 1). It has been previously reported that the isoelectric point (pI) is a significant indicator of protein stability and solubility, with an acidic pI contributing to enhanced protein integrity [43]. Overall, these parameters clearly suggest that both intimin and invasin possess highly stable structures.

4.4. Incongruency of *A. hydrophila* Invasin and Intimin with Existing Models

In the present investigation, both invasin and intimin were found to be composed of N-terminal Ig-like domains to create an appropriate rod length, as well as a C-terminal lectin-like domain (Figure 2A,B). This observation aligns with previous findings on the crystal structure of intimin from enteropathogenic *E. coli*, which similarly demonstrated a predominance of α -helices and extended strands without β -turns [44]. Experimental evidence from invasin in *Yersinia* and *Escherichia coli* shows a topology comprising a 12-stranded β -barrel with an α -helical linker located in the pore of the barrel, in analogy to classical autotransporters but with an inverted N- to C-terminal domain order [45]. The crystal structures of intimin and invasin from both enterohemorrhagic *E. coli* and *Yersinia*

pseudotuberculosis, specifically their translocation units, confirmed the topology model of a 12-stranded β -barrel with an α -helical linker residing in the predominantly hydrophilic pore [17].

4.5. Structural Stability and Diversity of Rohu Fish β -Integrins

The molecular cloning and sequence characterization of the β 1 integrin from *Cyprinus carpio* have been previously reported [46], yet there is limited information available regarding the molecular structure of fish integrins [47]. This study provides the comprehensive physicochemical characterization of all β -integrins in rohu. The β -integrins in rohu exhibit comparatively low AI values (β 2: 70.90 to β 6: 78.31) and high instability indices (β 2: 32.88 to β 5: 46.39). Similar to the test proteins, they also show negative GRAVY scores but have higher pI values, ranging from 5.25 (β 3) to 6.56 (β 1) (Table 2). A protein with an instability index smaller than 40 is generally predicted to be stable, indicating that, while some β -integrins may be less stable, they still exhibit features that could suggest functionality within their physiological context.

In eukaryotes, integrins represent a diverse family of cell adhesion receptors that play a crucial role in various biological processes, including cell signaling, immune responses, and tissue repair. This family consists of eight β -subunits and eight α -subunits, which non-covalently associate to form 24 distinct $\alpha\beta$ integrin heterodimers. Each β -subunit can bind to multiple α -subunits, allowing for a vast array of integrin combinations. Both the α - and β -subunits are type I transmembrane receptors that have a cytoplasmic tail, a single transmembrane domain, and a sizable extracellular region in common [48]. All β -integrins contain an inserted domain (I domain), which is homologous to the von Willebrand factor A domain (vWFA). In the phylogenetic tree based on the sequences of β -integrins, the vertebrate sequences form two major branches: group A includes β 1, β 2, and β 7, while group B comprises β 3, β 5, β 6, and β 8 [49]. Fish integrins are relatively less studied compared to mammalian integrins, particularly in humans. No crystal structures are available for rohu β -integrins. Huhtala et al. (2005) identified eight β -integrins in puffer fish, noting the absence of β 2 and β 7 orthologs of human β -integrins, while observing duplications of the β 1 and β 3 orthologs [50]. In contrast, our current findings reveal that the eight β -integrins of rohu are indeed orthologs of human β -integrins, suggesting a more complete representation of the integrin diversity in this species.

4.6. Binding of *A. hydrophila* Invasin and Intimin with Host Proteins

Invasin and intimin are bacterial Ig-like adhesins known as reverse autotransporters. It has been already demonstrated that, on supported lipid bilayers with diffusive intimin, Tir-expressing fibroblasts formed Tir–intimin clusters, whereas Tir tyrosine phosphorylation is necessary for actin polymerization from clusters [51]. In general, intimin and invasin are crucial proteins in bacterial pathogenesis, and their high-affinity binding is essential for bacterial attachment to host cells and for their subsequent internalization [52]. However, cognate host partner proteins of invasin are still unidentified [53]. The present molecular docking experiments reveal that rohu β -integrins (β 1– β 8), as receptors, exhibit strong binding affinity for *A. hydrophila* invasin (Figure 4A(a–h)) and intimin (Figure 4B(a–h)), suggesting a potential molecular mechanism for bacterial adhesion and invasion. In the current study, the docking scores for the experimental models ranged from -405.89 to -246.23 , reflecting strong binding potential. Additionally, the confidence scores, which ranged from 0.8734 to 0.9832, further support the likelihood of binding. In general, scores above 0.7 suggest a high probability of interaction. These findings indicate that both invasin and intimin from *A. hydrophila* exhibit robust binding affinity to all β -integrin members of rohu fish. Such high-affinity interactions are likely crucial for bacteria's attachment to the

extracellular matrix and in facilitating cell–cell interactions with the host [54]. Previous studies have also demonstrated similar tight binding, such as the interaction of invasin and intimin from *Y. enterocolitica* with the β 1 integrin in humans, underscoring the importance of these adhesin proteins in bacterial pathogenesis [55]. Invasin may recognize an unglycosylated region of integrins [56]. According to Leong et al. (1993), the disulfide bond between cysteines is required for integrin binding because it is necessary for proper folding [57]. On the other hand, Hamburger et al. (1999) showed that aspartic acid residues in invasin D5 in *Y. pseudotuberculosis* are required for integrin binding [56]. In the present investigation, the invasin protein of *A. hydrophila* ATCC 7966 exhibited varying numbers of aspartic acid residues across its different domains. Specifically, domain D5 contains five aspartic acid residues; D4 has eight residues; D3, which has the highest number, contains 17 aspartic acid residues; D2 comprises nine residues; and D1 holds six residues. These variations in the number of aspartic acid residues across different domains may play a significant role in the protein's structural stability and functional properties (Table 1). Similarly, in *A. hydrophila* ATCC 7966, the intimin protein contains aspartic acid residues distributed as follows: D3 has 8, D2 has 10, D1 has 7, and D0 has 6. This underscores the evolutionary conservation of the binding mechanisms among various pathogens targeting integrin receptors, which could contribute to the development of therapeutic strategies for bacterial infections in both aquatic and terrestrial hosts.

5. Conclusions

The selective presence of invasin and intimin in hypervirulent strains of *A. hydrophila*, coupled with their strong binding affinity to all eight β -integrins of rohu, emphasizes their pivotal role in disease progression. This specificity suggests that only certain strains of *A. hydrophila* possess the crucial molecular tools needed for effective interaction with host cells, thus facilitating efficient adhesion and invasion. We strongly believe that this information could provide valuable insights into the colonization process of this pathogen and its subsequent role in disease development.

Supplementary Materials: The following supporting information can be downloaded at: <https://www.mdpi.com/article/10.3390/bacteria4010007/s1>, Table S1: The accession numbers and DNA and protein sequences of the test proteins (invasin, and intimin) of *A. hydrophila* ATCC 7966; Table S2: Results of microbial genome BLAST for invasin and intimin within the *A. hydrophila* genomes using the tBLASTn algorithm; Table S3: Secondary structure prediction of invasin and intimin of *A. hydrophila* ATCC 7966; Table S4: Secondary structure prediction of β -integrins of rohu (*Labeo rohita*); Table S5: Functional analysis of invasin and intimin of *A. hydrophila* ATCC 7966; Table S6: Functional analysis of β -integrins of rohu (*Labeo rohita*); Table S7: Homology modeling data of invasin and intimin of *A. hydrophila* by SWISS-MODEL accessed via the ExPASy web server; Table S8: Homology modeling of the β -integrins of rohu (*Labeo rohita*) by SWISS-MODEL accessed via the ExPASy web server; Table S9: Evaluation of tertiary structure of invasin and intimin of *A. hydrophila* by SWISS-MODEL accessed via the ExPASy web server; Table S10: Evaluation of tertiary structure of β -integrins of rohu (*Labeo rohita*) by SWISS-MODEL accessed via the ExPASy web server; Table S11: Evaluation of receptor–ligand interface residue pair(s); Figure S1: Secondary structure analysis of (A) invasin and (B) intimin of *A. hydrophila* ATCC 7966 through SOPMA; Figure S2: Secondary structure analysis of β -integrins 1 to 8 (a, b, c, d, e, f, g, and h) of *L. rohita* through SOPMA; Figure S3: Homology modeling of β -integrins of *L. rohita* by SWISS-MODEL, accessed via the ExPASy web server. Figure S4: Evaluation of tertiary structures of the β Integrins –1 to –8 (a, b, c, d, e, f, g, and h) of *L. rohita*. In each panel, (a) represents Z- scores in terms of residues, (b) represents sequence position, (c) represents Ramachandran plot, (d) represents hydrophobicity, and (e) represents net charge density.

Author Contributions: Conceptualization, G.B. and P.C.; methodology, A.B. and P.C.; software, A.B., G.B. and P.C.; formal analysis, A.B., G.B. and P.C.; investigation, P.C.; resources, G.B. and P.C.; data curation, A.B. and P.C.; writing—original draft preparation, A.B., G.B. and P.C.; writing—review and editing, G.B. and P.C.; visualization, A.B. and P.C.; supervision, P.C.; project administration, P.C. All authors have read and agreed to the published version of the manuscript.

Funding: This work is not funded by any agencies.

Institutional Review Board Statement: Not applicable.

Informed Consent Statement: Not applicable.

Data Availability Statement: All data are available in public databases, including the KEGG Orthology database (<https://www.genome.jp/kegg/ko.html> last accessed on 31 March 2024), UniProt database (<https://www.uniprot.org/> last accessed on 31 March 2024), and NCBI Genome database (<https://www.ncbi.nlm.nih.gov/genome> last accessed on 31 March 2024).

Acknowledgments: We are grateful to Raja Rammohun Roy Mahavidyalaya and M.U.C. Women's College, India, as well as the University of Illinois, Urbana-Champaign, Illinois, USA, for providing the necessary resources and support for this study. This research received no external funding.

Conflicts of Interest: The authors declare no conflicts of interest.

References

1. Harikrishnan, R.; Balasundaram, C. Modern Trends in *Aeromonas hydrophila* Disease Management with Fish. *Rev. Fish. Sci.* **2005**, *13*, 281–320. [[CrossRef](#)]
2. Chang, P.; Wu, T.; Chung, H.; Chien, C. *Aeromonas hydrophila* and *Saprolegnia australis* Isolated from Ayu, *Plecoglossus altivelis* with Ulcerative Skin Disease in Taiwan. *Bull. Eur. Assoc. Fish Pathol.* **2002**, *22*, 393–399.
3. Cipriano, R.C. *Aeromonas hydrophila* and Motile *Aeromonad* Septicemias of Fish; US Department of the Interior, Fish and Wildlife Service, Division of Fishery Research: Washington, DC, USA, 1984; Volume 68.
4. Citterio, B.; Biavasco, F. *Aeromonas hydrophila* virulence. *Virulence* **2015**, *6*, 417–418. [[CrossRef](#)] [[PubMed](#)]
5. Rahayu, K.; Daruti, D.; Stella, M. Study on Characterization, Pathogenicity and Histopathology of Disease Caused by *Aeromonas hydrophila* in gourami (*Osphronemus gouramy*). *IOP Conf. Ser. Earth Environ. Sci.* **2018**, *137*, 012003.
6. Yardımcı, B.; Aydın, Y. Pathological Findings of Experimental *Aeromonas hydrophila* infection in Nile Tilapia (*Oreochromis niloticus*). *Ank. Üniversitesi Vet. Fakültesi Derg.* **2011**, *58*, 47–54.
7. Grizzle, J.M.; Kiryu, Y. Histopathology of Gill, Liver, and Pancreas, and Serum Enzyme Levels of Channel Catfish Infected with *Aeromonas hydrophila* Complex. *J. Aquat. Anim. Health* **1993**, *5*, 36–50. [[CrossRef](#)]
8. Sarker, J.; Faruk, M. Experimental Infection of *Aeromonas hydrophila* in Pangasius. *Progress. Agric.* **2016**, *27*, 392–399. [[CrossRef](#)]
9. Di, J.; Zhang, S.; Huang, J.; Du, H.; Zhou, Y.; Zhou, Q.; Wei, Q. Isolation and Identification of Pathogens Causing Haemorrhagic Septicaemia in Cultured Chinese Sturgeon (*Acipenser sinensis*). *Aquac. Res.* **2018**, *49*, 3624–3633. [[CrossRef](#)]
10. Barde, R.D. Exploring the Disease-Causing Potential of *Aeromonas Hydrophila* Obtained from Freshwater Carp-*Cirrhinus mrigala*. *J. Surv. Fish. Sci.* **2023**, *10*, 1725–1732.
11. Saier, M.H.; Ma, C.H.; Rodgers, L.; Tamang, D.G.; Yen, M.R.; Laskin, A.; Sariaslani, S.; Gadd, G. Protein Secretion and Membrane Insertion Systems in Bacteria and Eukaryotic Organelles. *Adv. Appl. Microbiol.* **2008**, *65*, 141–197. [[PubMed](#)]
12. Newman, C.L.; Stathopoulos, C. Autotransporter and Two-Partner Secretion: Delivery of Large-Size Virulence Factors by Gram-Negative Bacterial Pathogens. *Crit. Rev. Microbiol.* **2004**, *30*, 275–286. [[CrossRef](#)] [[PubMed](#)]
13. Meuskens, I.; Saragliadis, A.; Leo, J.C.; Linke, D. Type V Secretion Systems: An Overview of Passenger Domain Functions. *Front. Microbiol.* **2019**, *10*, 1163. [[CrossRef](#)] [[PubMed](#)]
14. Isberg, R.R.; Leong, J.M. Multiple β 1 Chain Integrins Are Receptors for Invasin, a Protein That Promotes Bacterial Penetration Into Mammalian Cells. *Cell* **1990**, *60*, 861–871. [[CrossRef](#)] [[PubMed](#)]
15. Gal-Mor, O.; Gibson, D.L.; Baluta, D.; Vallance, B.A.; Finlay, B.B. A Novel Secretion Pathway of *Salmonella enterica* Acts as an Antivirulence Modulator During Salmonellosis. *PLoS Pathog.* **2008**, *4*, e1000036. [[CrossRef](#)]
16. Kang, S.; Ryu, S.; Chae, J.; Eo, S.; Woo, G.; Lee, J. Occurrence and Characteristics of Enterohemorrhagic *Escherichia coli* O157 in Calves Associated with Diarrhoea. *Vet. Microbiol.* **2004**, *98*, 323–328. [[CrossRef](#)] [[PubMed](#)]
17. Fairman, J.W.; Dautin, N.; Wojtowicz, D.; Liu, W.; Noinaj, N.; Barnard, T.J.; Udho, E.; Przytycka, T.M.; Cherezov, V.; Buchanan, S.K. Crystal Structures of the Outer Membrane Domain of Intimin and Invasin From Enterohemorrhagic *E. coli* and Enteropathogenic *Y. pseudotuberculosis*. *Structure* **2012**, *20*, 1233–1243. [[CrossRef](#)] [[PubMed](#)]

18. Ruoslahti, E. RGD and Other Recognition Sequences for Integrins. *Annu. Rev. Cell Dev. Biol.* **1996**, *12*, 697–715. [[CrossRef](#)]
19. Holmes, R.S.; Rout, U.K. Comparative Studies of Vertebrate Beta Integrin Genes and Proteins: Ancient Genes in Vertebrate Evolution. *Biomolecules* **2011**, *1*, 3–31. [[CrossRef](#)]
20. Xiong, J.-P.; Stehle, T.; Diefenbach, B.; Zhang, R.; Dunker, R.; Scott, D.L.; Joachimiak, A.; Goodman, S.L.; Arnaout, M.A. Crystal Structure of the Extracellular Segment of Integrin $\alpha V\beta 3$. *Science* **2001**, *294*, 339–345. [[CrossRef](#)]
21. Takada, Y.; Ye, X.; Simon, S. The Integrins. *Genome Biol.* **2007**, *8*, 215. [[CrossRef](#)] [[PubMed](#)]
22. Watarai, M.; Funato, S.; Sasakawa, C. Interaction of Ipa Proteins of *Shigella flexneri* with Alpha5beta1 Integrin Promotes Entry of the Bacteria Into Mammalian Cells. *J. Exp. Med.* **1996**, *183*, 991–999. [[CrossRef](#)]
23. Leong, J.M.; Fournier, R.S.; Isberg, R. Identification of the Integrin Binding Domain of the *Yersinia pseudotuberculosis* Invasin Protein. *EMBO J.* **1990**, *9*, 1979–1989. [[CrossRef](#)]
24. Isberg, R.R.; Van Nhieu, G.T. Binding and Internalization of Microorganisms by Integrin Receptors. *Trends Microbiol.* **1994**, *2*, 10–14. [[CrossRef](#)]
25. François-Étienne, S.; Nicolas, L.; Eric, N.; Jaqueline, C.; Pierre-Luc, M.; Sidki, B.; Aleicia, H.; Danilo, B.; Luis, V.A.; Nicolas, D. Important Role of Endogenous Microbial Symbionts of Fish Gills in the Challenging but Highly Biodiverse Amazonian Blackwaters. *Nat. Commun.* **2023**, *14*, 3903. [[CrossRef](#)]
26. Oberto, J. SyntTax: A Web Server Linking Synteny to Prokaryotic Taxonomy. *BMC Bioinform.* **2013**, *14*, 4. [[CrossRef](#)]
27. Lovell, S.C.; Davis, I.W.; Arendall, W.B., III; De Bakker, P.I.; Word, J.M.; Prisant, M.G.; Richardson, J.S.; Richardson, D.C. Structure Validation by C α Geometry: ϕ , Ψ and C β Deviation. *Proteins Struct. Funct. Bioinform.* **2003**, *50*, 437–450. [[CrossRef](#)]
28. Ramachandran, G. Molecular Structure of Collagen. *Int. Rev. Connect. Tissue Res.* **1963**, *1*, 127–182.
29. Yan, Y.; Zhang, D.; Zhou, P.; Li, B.; Huang, S.-Y. Hdock: A Web Server for Protein–Protein and Protein–DNA/RNA Docking Based on a Hybrid Strategy. *Nucleic Acids Res.* **2017**, *45*, W365–W373. [[CrossRef](#)] [[PubMed](#)]
30. Schmidt, M.A. LEEways: Tales of EPEC, ATEC and EHEC. *Cell. Microbiol.* **2010**, *12*, 1544–1552. [[CrossRef](#)]
31. Tsai, J.C.; Yen, M.-R.; Castillo, R.; Leyton, D.L.; Henderson, I.R.; Saier, M.H., Jr. The Bacterial Intimins and Invasins: A Large and Novel Family of Secreted Proteins. *PLoS ONE* **2010**, *5*, e14403. [[CrossRef](#)]
32. Leo, J.C.; Oberhettinger, P.; Schütz, M.; Linke, D. The Inverse Autotransporter Family: Intimin, Invasin and Related Proteins. *Int. J. Med. Microbiol.* **2015**, *305*, 276–282. [[CrossRef](#)] [[PubMed](#)]
33. Bhattacharyya, A.; Banerjee, G.; Chattopadhyay, P. Probable Role of Type IV Pili of *Aeromonas hydrophila* in Human Pathogenicity. *Pathogens* **2024**, *13*, 365. [[CrossRef](#)] [[PubMed](#)]
34. Xu, T.; Rasmussen-Ivey, C.R.; Moen, F.S.; Fernández-Bravo, A.; Lamy, B.; Beaz-Hidalgo, R.; Khan, C.D.; Castro Escarpulli, G.; Yasin, I.S.M.; Figueras, M.J. A Global Survey of Hypervirulent *Aeromonas hydrophila* (Vah) Identified Vah Strains in the Lower Mekong River Basin and Diverse Opportunistic Pathogens from Farmed Fish and Other Environmental Sources. *Microbiol. Spectr.* **2023**, *11*, e03705-22. [[CrossRef](#)] [[PubMed](#)]
35. Shea, A.E.; Stocki, J.A.; Himpsl, S.D.; Smith, S.N.; Mobley, H.L. Loss of an Intimin-Like Protein Encoded on a Uropathogenic *E. coli* Pathogenicity Island Reduces Inflammation and Affects Interactions with the Urothelium. *Infect. Immun.* **2022**, *90*, e00275-21. [[CrossRef](#)] [[PubMed](#)]
36. Jackson-Litteken, C.D.; Di Venanzio, G.; Le, N.-H.; Scott, N.E.; Djahanschiri, B.; Distel, J.S.; Pardue, E.J.; Ebersberger, I.; Feldman, M.F. InvL, an Invasin-Like Adhesin, Is a Type II Secretion System Substrate Required for *Acinetobacter baumannii* Uropathogenesis. *MBio* **2022**, *13*, e00258-22. [[CrossRef](#)] [[PubMed](#)]
37. Hamburger, Z.A. Crystallographic Studies of Invasin, a Bacterial Adhesion Molecule from *Yersinia pseudotuberculosis*. Ph.D. Thesis, California Institute of Technology, Pasadena, CA, USA, 2002.
38. Martinez-Gil, M.; Goh, K.G.; Rackaityte, E.; Sakamoto, C.; Audrain, B.; Moriel, D.G.; Totsika, M.; Ghigo, J.-M.; Schembri, M.A.; Beloin, C. YeeJ Is an Inverse Autotransporter from *Escherichia coli* that Binds to Peptidoglycan and Promotes Biofilm Formation. *Sci. Rep.* **2017**, *7*, 11326. [[CrossRef](#)]
39. Goh, K.G.; Moriel, D.G.; Hancock, S.J.; Phan, M.-D.; Schembri, M.A. Bioinformatic and Molecular Analysis of Inverse Autotransporters from *Escherichia coli*. *MSphere* **2019**, *4*. [[CrossRef](#)] [[PubMed](#)]
40. Sinclair, J.F.; O'Brien, A.D. Intimin types α , β , and Γ Bind to Nucleolin with Equivalent Affinity but Lower Avidity Than to the Translocated Intimin Receptor. *J. Biol. Chem.* **2004**, *279*, 33751–33758. [[CrossRef](#)] [[PubMed](#)]
41. Panda, S.; Chandra, G. Physicochemical Characterization and Functional Analysis of Some Snake Venom Toxin Proteins and Related Non-Toxin Proteins of Other Chordates. *Bioinformation* **2012**, *8*, 891. [[CrossRef](#)]
42. Enany, S. Structural and Functional Analysis of Hypothetical and Conserved Proteins of *Clostridium tetani*. *J. Infect. Public Health* **2014**, *7*, 296–307. [[CrossRef](#)]
43. Tokmakov, A.A.; Kurotani, A.; Sato, K.-I. Protein pI and Intracellular Localization. *Front. Mol. Biosci.* **2021**, *8*, 775736. [[CrossRef](#)]
44. Luo, Y.; Frey, E.A.; Pfuetzner, R.A.; Creagh, A.L.; Knoechel, D.G.; Haynes, C.A.; Finlay, B.B.; Strynadka, N.C. Crystal Structure of Enteropathogenic *Escherichia coli* Intimin–Receptor Complex. *Nature* **2000**, *405*, 1073–1077. [[CrossRef](#)] [[PubMed](#)]

45. Oberhettinger, P.; Schütz, M.; Leo, J.C.; Heinz, N.; Berger, J.; Autenrieth, I.B.; Linke, D. Intimin and Invasin Export Their C-Terminus to the Bacterial Cell Surface Using an Inverse Mechanism Compared to Classical Autotransport. *PLoS ONE* **2012**, *7*, e47069. [[CrossRef](#)]
46. Jiang, X.; Sun, J.; Li, C.; Hu, X.; Ge, Y.; Li, B.; Shi, L.; Jia, Z. Molecular Cloning and Sequence Characterization of Common Carp (*Cyprinus carpio*) Integrin B1 (Itg β 1) and Its Temporal Expression in Response to CyHV-3. *Aquac. Int.* **2021**, *29*, 1869–1884. [[CrossRef](#)]
47. Xiong, X.; Yang, H.; Ding, C.; Qin, B.; Deng, Y.; Xiong, L.; Liu, X.; Li, Y.; Xiao, T.; Lv, Z. Functional and Expression Analysis Reveals the Involvement of Integrin Av β 3 in Antiviral Immunity of Grass Carp (*Ctenopharyngodon idella*). *Fish Shellfish Immunol.* **2022**, *129*, 52–63. [[CrossRef](#)] [[PubMed](#)]
48. Xiao, T.; Takagi, J.; Coller, B.S.; Wang, J.-H.; Springer, T.A. Structural Basis for Allostery in Integrins and Binding to Fibrinogen-mimetic Therapeutics. *Nature* **2004**, *432*, 59–67. [[CrossRef](#)] [[PubMed](#)]
49. Hughes, A.L. Evolution of the Integrin α and β Protein Families. *J. Mol. Evol.* **2001**, *52*, 63–72. [[CrossRef](#)]
50. Huhtala, M.; Heino, J.; Casciari, D.; de Luise, A.; Johnson, M.S. Integrin Evolution: Insights from Ascidian and Teleost Fish Genomes. *Matrix Biol.* **2005**, *24*, 83–95. [[CrossRef](#)]
51. Oh, D.; Liu, X.; Sheetz, M.P.; Kenney, L.J. Small, Dynamic Clusters of Tir-Intimin Seed Actin Polymerization. *Small* **2023**, *19*, 2302580. [[CrossRef](#)]
52. Tran Van Nhieu, G.; Isberg, R.R. Bacterial Internalization Mediated by Beta 1 Chain Integrins Is Determined by Ligand Affinity and Receptor Density. *EMBO J.* **1993**, *12*, 1887–1895. [[CrossRef](#)] [[PubMed](#)]
53. Chatterjee, S.; Basak, A.J.; Nair, A.V.; Duraivelan, K.; Samanta, D. Immunoglobulin-Fold Containing Bacterial Adhesins: Molecular and Structural Perspectives in Host Tissue Colonization And Infection. *FEMS Microbiol. Lett.* **2021**, *368*, fnaa220. [[CrossRef](#)]
54. Isberg, R.R.; Hamburger, Z.; Dersch, P. Signaling and Invasin-Promoted Uptake via Integrin Receptors. *Microbes Infect.* **2000**, *2*, 793–801. [[CrossRef](#)] [[PubMed](#)]
55. Rakin, A.; Garzetti, D.; Bouabe, H.; Sprague, L.D. *Yersinia enterocolitica*. In *Molecular Medical Microbiology*; Elsevier: Amsterdam, The Netherlands, 2015; pp. 1319–1344.
56. Hamburger, Z.A.; Brown, M.S.; Isberg, R.R.; Bjorkman, P.J. Crystal Structure of Invasin: A Bacterial Integrin-Binding Protein. *Science* **1999**, *286*, 291–295. [[CrossRef](#)]
57. Leong, J.; Morrissey, P.; Isberg, R. A 76-Amino Acid Disulfide Loop in the *Yersinia pseudotuberculosis* Invasin Protein Is Required for Integrin Receptor Recognition. *J. Biol. Chem.* **1993**, *268*, 20524–20532. [[CrossRef](#)]

Disclaimer/Publisher’s Note: The statements, opinions and data contained in all publications are solely those of the individual author(s) and contributor(s) and not of MDPI and/or the editor(s). MDPI and/or the editor(s) disclaim responsibility for any injury to people or property resulting from any ideas, methods, instructions or products referred to in the content.